



**AIAA-2005-2383**

**Orbital Debris Shape and Orientation Effects on Ballistic Limits**

S. Evans

NASA-Marshall Space Flight Center

Huntsville, AL

and

J. Williamsen

Institute for Defense Analyses

Alexandria, VA

**46<sup>th</sup> Structures, Structural Dynamics, and Materials  
Conference  
18-21 April, 2005  
Austin, TX**

For permission to copy or republish, contact the copyright owner named on the first page.

For AIAA-held copyright, write to AIAA Permissions Department,

1801 Alexander Bell Drive, Suite 500, Reston, VA, 20191-4344.



Figure 2 shows the simulation setups for a sphere and a flake, both with  $L_c = 0.6$  cm. The sphere's mass was 0.314 g, and the flake's was 0.115 g. The flake setup corresponds to the "Face A-B (45-45)" example in Figure 1. Figure 3 compares the debris clouds of these simulations at 8 microseconds into the events. The flake's debris cloud lacks the low-density lead element of the sphere's, and has a concentration of dense material in an arc at approximately the vertical location of the sphere's central fragment mass. This arc is aligned along what were the normals to the flake's largest (square) faces. Nestled in the center of the arc is a barely-fractured remnant of the trailing corner of the flake. The development of this arc structure along the flake face normals is seen in debris clouds from other orientations as well. Figure 4 compares the backwall damage due to these projectiles at the 100 microsecond point. While both projectiles fail the backwall, the damage characteristics are distinctly different. The sphere produces a collection of small perforations near the center of the backwall, several of whose margins have coalesced to make what should develop into a set of jagged petals at later times. The flake produces a lenticular rip in the backwall, aligned with the dense debris arc and flake face normal line. Such a linear hole might cause the backwall to be more subject to an "unzipping" failure at later times if it happened to fall near the wall's principle stress axis. At this stage the flake's hole size is several times that of the sphere's for this orientation, but whether this difference is maintained at later times is unknown.

Hu and Schonberg (Ref. 4) reported that non-spherical impactors were much more damaging than spherical impactors of the same mass. We concur in this finding, since the case above shows that a square flake can produce greater damage than a spherical impactor of over 2.5 times the mass. However, the quantity observed in the debris population is not mass, but RCS, which is directly related to  $L_c$ . We prefer to develop ballistic limits based on this observed variable, but owing to the constraints of time, we can only report results obtained at 12 km/s, comparing flakes to spheres.

Accordingly, we varied  $L_c$  for each of the five orientations shown in Figure 1, and recorded the  $L_c$  values for which the projectile produced four classes of backwall damage: clearly visible through-holes; spallation of SPH particles with accompanying backwall fracture, but no discernable through-holes; fractured back surface particles, but no spallation; and plastic deformation without fracture of the back surface. The  $L_c$  values, corresponding masses, and resulting damage are shown in Table 1. The  $L_c$  values in this table define a ballistic limit band applicable to these non-spherical particles at an impact speed of 12 km/s. The smallest values of  $L_c$  resulting in clearly visible perforations define an upper bound to this band, each applicable to its specific orientation. The largest values of  $L_c$  resulting in plastic-deformation-only define the lower bound of the band, again for each specific orientation. For each orientation the shift from fracture-only to production of through-holes constitutes a transition depending on the specifics of the simulation model and code – a modeling uncertainty. Considering all the orientation cases together, we observe a spread in the  $L_c$  values for the various types of damage that is greater than the spread for any given orientation. This spread constitutes an uncertainty band that depends on projectile orientation, convolved with the modeling uncertainty. By defining this wider band, we indicate an inherent uncertainty attached to any ballistic limit prediction that makes use of the SBM shape model. Thus, this uncertainty contributes to the damage uncertainty attachable to EVOLVE, and thence to the uncertainty in ORDEM2000.

Future work will extend the velocity range covered down to at least 7 km/s, and up to 15 km/s. Statistical methods will be applied to refine our statements about the uncertainty bands, and any variation of these bands with velocity.

## References

1. Williamsen, J. "Review of Space Shuttle Meteoroid/Orbital Debris Critical Risk Assessment Practices," IDA Paper P-3838, November 2003.
2. Reynold, R.C., et al. "NASA Standard Breakup Model, 1998 Revision." Lockheed Martin Space and Mission Systems and Services Report LMSMSS-32532, September 1998.
3. Evans, S., et al. "Comparison of SPHC Hydrocode Results with Penetration Equations and Results of Other Codes," AIAA 2004-1878, 45<sup>th</sup> SDM Conference, Palm Springs, CA, April 2004.
4. Hu, K., and Schonberg, W. P., "Ballistic Limit Curves for Non-Spherical Projectiles Impacting Dual-Wall Spacecraft Systems," Hypervelocity Impact Symposium, Noordwijk, Netherlands, December 2003.
5. Christiansen, E., and Kerr, J. "Ballistic Limit Equations for Spacecraft Shielding," *Int. J. Impact Engng.*, 2001; 26: 93-104.

Table 1: Flake impact aspect run matrix. Velocity 12 km/s, obliquity 1.6 deg.

"Edge-on" Cases			Lc (mm)	Mass (g)	Plastic Frac	Spall	Thru
Rx = 0 Ry = 0 Rz = 0	Rz = 0	4.0	4.0	0.039			
		4.5					
		5.0	4.0	0.071		X	
		5.5					
		6.0	4.0	0.115			X
	Rz = 45	4.0	4.0	0.039			
		4.5					
		5.0	4.0	0.071			
		5.5					
		6.0	4.0	0.115			
	Rz = 90	4.0	4.0	0.039	X		
		4.5					
		5.0	4.0	0.071			X
		5.5					
		6.0	4.0	0.115			X
"Corner-on" Cases							
Rx = 0 Ry = 45 Rz = 45	Rz = 45	4.0	4.0	0.039			
		4.5					
		5.0	4.0	0.071			
		5.5					
		6.0	4.0	0.115			
	Rz = 90	4.0	4.0	0.039			
		4.5					
		5.0	4.0	0.071			
		5.5					
		6.0	4.0	0.115			X
Sphere Cases							
		4.0	4.0	0.093		X	
		4.5					
		5.0					
		5.5					
		6.0	4.0	0.314			X

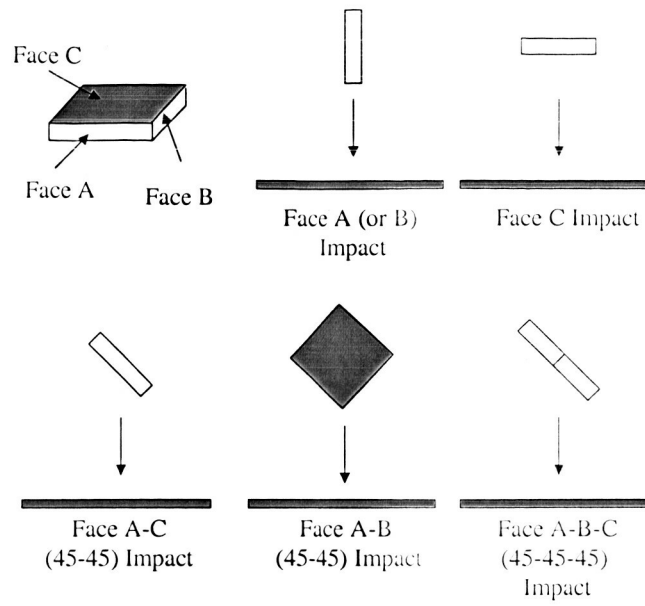


Figure 1: Impact flake geometry and impact orientations used in the simulations.

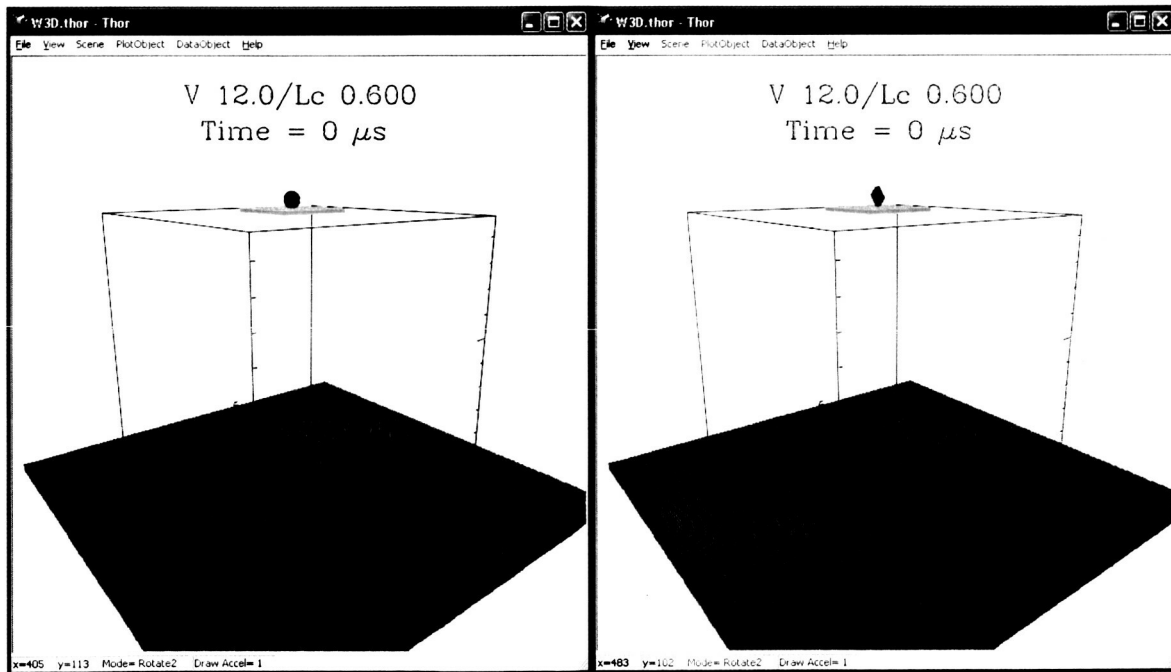


Figure 2: Sphere and flake setups, 3-D views.

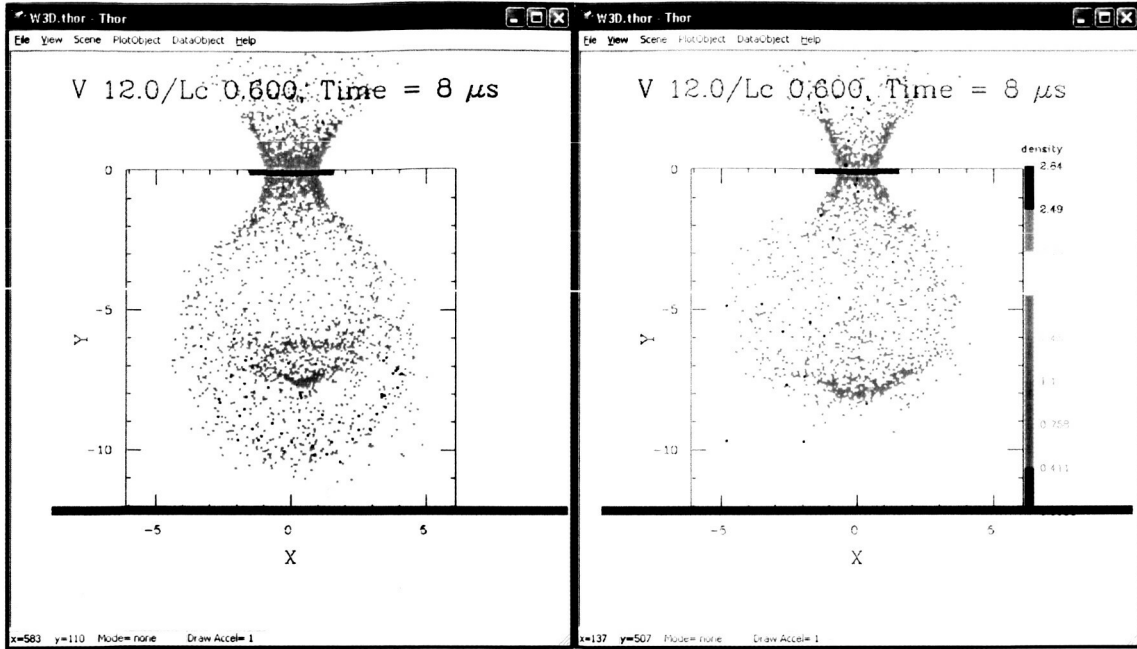


Figure 3: 2-D views of debris clouds of sphere (left) and flake (right).

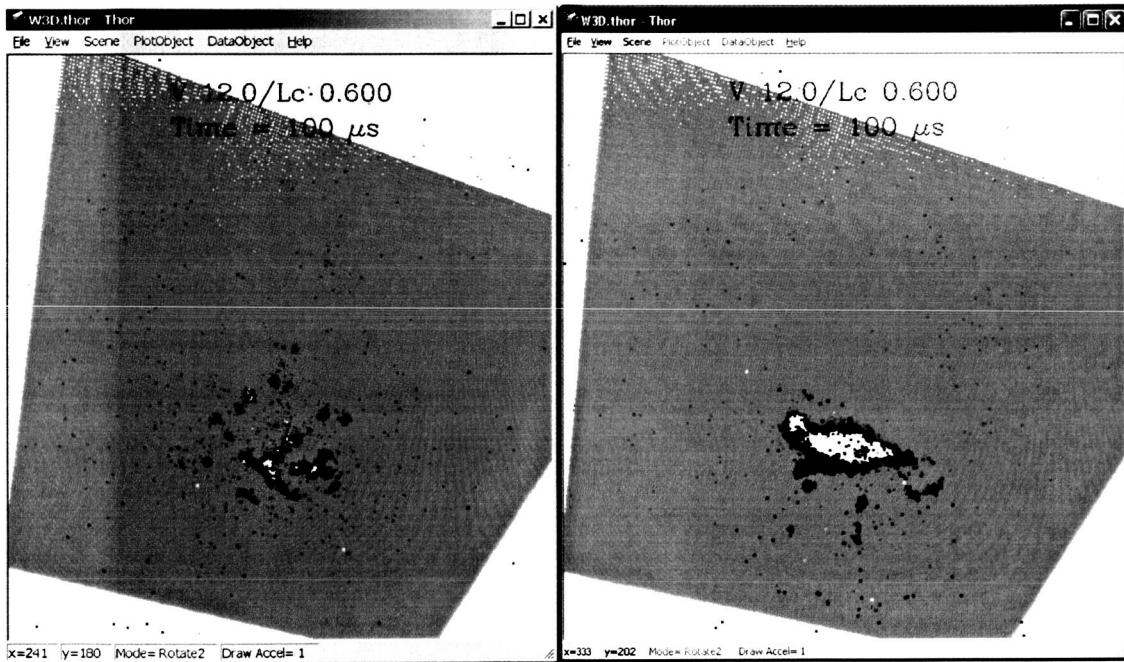


Figure 4: 3-D views of backwall damage by the sphere (left) and the flake (right); view is from behind the backwall. Dark blue material is fractured; light blue is plastically yielded; green is undisturbed solid. Through-holes are visible as white.